DESTRIPING AND INPAINTING OF REMOTE SENSING IMAGES USING MAXIMUM A-POSTERIORI METHOD

Huanfeng Shen [a, *], Tinghua Ai [a], Pingxiang Li [b]

[a] School of Resource and Environmental Science, Wuhan University, Wuhan 430079, China - shenhf@whu.edu.cn
[b] The State Key Laboratory of Information Engineering in Surveying, Mapping and Remote Sensing

Commission I, WG I/1

KEY WORDS: Correction, Retrieval, Algorithms, Image, Radiometric

ABSTRACT:

In a large number of spaceborne and airborne multi-detector spectrometer imagery, there commonly exist image stripes and random dead pixels. The techniques to recover the image from the contaminated one are called image destriping (for stripes) and image inpainting (for dead pixels). In order to constrain the solution space according to *a priori* knowledge, this paper presents a maximum *a posteriori* (MAP) based algorithm for both destriping and inpainting problems. In the MAP framework, the likelihood probability density function (PDF) is constructed based on a linear image observation model, and a robust Huber-Markov model is used as the prior PDF. A gradient descent optimization method is employed to produce the desired image. The proposed algorithm has been tested on images of different sensors. Experimental results show that it performs quite well in terms of both quantitative measurements and visual evaluation.

1. INTRODUCTION

Remote sensing images often suffer from the common problems of stripe noises and linear or random dead pixels. These severely degrade the quality of the measured imagery, and will introduce a considerable level of noise when processing data without correction of them. The correction of image stripes is commonly called as image destriping. The recovery of the dead pixels sometimes goes by the name of dead pixel replacement. In this paper, however, we use another more attractive name, i.e., image inpainting, which has been widely used in the field of digital image processing(Bertalmio et al., 2000).

At the highest level, destriping techniques can be divided into frequency domain or spatial domain algorithms. The simplest frequency domain algorithm is to process the image data with a low-pass filter using discrete Fourier transform (DFT). This method has the advantage of being usable on geo-rectified images, but it often does not remove all stripes and leads to significant blurring within the image. Chen et al. (Chen et al., 2003) proposed a method to distinguish the striping-induced frequency components using the power spectrum, and then remove the stripes using a power finite-impulse response filter. Some researchers remove the stripes using wavelet analysis which takes advantage of the scaling and directional properties to detect and eliminate striping patterns (Chen et al., 2006; Torres and Infante, 2001).

In the spatial domain, most destriping algorithms examine the distribution of digital numbers for each sensor, and adjusts this distribution to some reference distribution (Gadallah et al., 2000). These methods are equalization(Algazi and G. E. Ford, 1981), histogram matching (Horn and Woodham, 1979; Wegener, 1990), moment matching (Gadallah et al., 2000), and others. More recently, Rakwatin et al. (Rakwatin et al., 2007) combined histogram matching with facet filter for stripe noise reduction in MODIS data. These methods have a similarity assumption for the image data.

For the inpainting problem, the nearest-neighbor, average or median value replacement methods are commonly employed (Ratliff et al., 2007). The main disadvantage of these methods is that they are employable only when the dead area is small (for example, the width of the dead line is only one or two pixels). Even for dead areas just a little larger, these methods will produce obvious artifacts.

In this paper, we formulate the destriping and inpainting problems using Maximum *A Posteriori* (MAP) estimation. Our motivation is to constrain the solution space of the ill-posed problems according to *a priori* knowledge on the form of the solution using the MAP framework. To our best knowledge, this is the first time that remote sensing destriping or inpainting problem is formulated using probabilistic approach.

2. THE PROPOSED ALGORITHM

2.1 Image Observation Model

Letting $z_{x,y}$ and $g_{x,y}$ respectively denote the input radiance to be measured and the senor output of location (x, y), the relationship between $z_{x,y}$ and $g_{x,y}$ can be related by a linear or nonlinear function. In this paper, we assume the degradation process can be linearly described as in (Gadallah et al., 2000;

* Corresponding author.

Poros and Peterson, 1985), but we permit the existence of linear-assumption error as

$$g_{x,y} = A_{x,y} z_{x,y} + B_{x,y} + n_{x,y} \quad (1)$$

where $A_{x,y}$ and $B_{x,y}$ are the relative gain and offset parameters respectively, $n_{x,y}$ is the sum of linear-assumption error and sensor noise. In matrix-vector form, the relation between the observed image and the desired image can be expressed as

$$\boldsymbol{g} = \boldsymbol{A}\boldsymbol{z} + \boldsymbol{B} + \boldsymbol{n} \quad (2)$$

In the model, $\boldsymbol{g}$ is the lexicographically ordered vector of the observed image, $\boldsymbol{z}$ represents the desired image, $\boldsymbol{A}$ is a diagonal matrix with diagonal elements being the gains of all pixels, $\boldsymbol{B}$ is the offset vector, and $\boldsymbol{n}$ represents the noise vector.

2.2 MAP Reconstruction Model

In recent years, the Maximum *A Posteriori* (MAP) estimation method has been central to the solution of ill-posed inverse problems in a wide range of applications (Borman and Stevenson, 1998), such as image denoising (Hamza and Krim, 2004), deblurring (Ferrari et al., 1995), super resolution reconstruction (Shen et al., 2007), and others. Our purpose is to realize the MAP estimate of a destriped or inpainted image $\boldsymbol{z}$, given the degraded image $\boldsymbol{g}$. It can be computed by

$$\hat{\boldsymbol{z}} = \arg\max_{\boldsymbol{z}} p(\boldsymbol{z} \mid \boldsymbol{g}) . \quad (3)$$

Applying Bayes' rule, equation (3) becomes

$$\hat{\boldsymbol{z}} = \arg\max_{\boldsymbol{z}} \frac{p(\boldsymbol{g} \mid \boldsymbol{z}) p(\boldsymbol{z})}{p(\boldsymbol{g})} . \quad (4)$$

Since $p(\boldsymbol{z} \mid \boldsymbol{g})$ is independent of $\boldsymbol{g}$, $p(\boldsymbol{g})$ can be considered a constant and hence equation (4) can be rewritten as

$$\hat{\boldsymbol{z}} = \arg\max_{\boldsymbol{z}} p(\boldsymbol{g} \mid \boldsymbol{z}) p(\boldsymbol{z}) . \quad (5)$$

The first probability density functions (PDF) in (5) is the likelihood density function. It is determined by the probability density of the noise vector in (2), i.e., $p(\boldsymbol{g} \mid \boldsymbol{z}) = p(\boldsymbol{n})$. Since different pixels may be degraded to different degrees in the destriping and inpainting problems, we assume the noise is not identical, but still independent. Under these assumptions, the probability density is given by

$$p(\boldsymbol{g} \mid \boldsymbol{z}) = \frac{1}{M_1} \exp\left\{ -\frac{1}{2} (\boldsymbol{g} - \boldsymbol{A}\boldsymbol{z} - \boldsymbol{B})^T \boldsymbol{K}^{-1} (\boldsymbol{g} - \boldsymbol{A}\boldsymbol{z} - \boldsymbol{B}) \right\} \quad (6)$$

where M_1 is a constant, and $\boldsymbol{K}$ is the covariance matrix that describes the noise. Since the noise is assumed independent, $\boldsymbol{K}$ is a diagonal matrix containing the noise variances. Thus, we can further rewrite equation (6) as

$$p(\boldsymbol{g} \mid \boldsymbol{z}) = \frac{1}{M_1} \exp\left\{ -\frac{1}{2} \left\| \boldsymbol{Q}(\boldsymbol{g} - \boldsymbol{A}\boldsymbol{z} - \boldsymbol{B}) \right\|^2 \right\} \quad (7)$$

where $\boldsymbol{Q}$ is also a diagonal matrix.

The second density function in (5) is the image prior which imposes the spatial constrains on the image. This may include such constraints such as positivity, smoothness and so on. Here, we employ an edge-preserving Huber-Markov image prior model. This prior model can effectively preserve the edge and detailed information in the image (Schultz and Stevenson, 1996; Shen et al., 2007, doi:10.1093/comjnl/bxm028). It is denoted as

$$p(\boldsymbol{z}) = \frac{1}{M_2} \exp\left(-\frac{1}{2\lambda} \sum_{x,y} \sum_{c \in C} \rho(d_c(z_{x,y})) \right) \quad (8)$$

In this expression, M_2 is a constant, c is a clique within the set of all image cliques C, the quantity $d_c(z_{x,y})$ is a spatial activity measure to pixel $z_{x,y}$ which is often formed by first-order or second-order differences, and $\rho(\cdot)$ is a Huber function defined as

$$\rho(i) = \begin{cases} i^2 & |i| \le \mu \\ 2\mu |i| - \mu^2 & |i| > \mu \end{cases} \quad (9)$$

where μ is a threshold parameter separating the quadratic and linear regions.

As for the $d_c(z_{x,y})$, we compute the following finite second-order differences in four adjacent cliques for every location (x, y) in the image

$$d_c^1(z_{x,y}) = z_{x-1,y} - 2z_{x,y} + z_{x+1,y} \quad (10)$$

$$d_c^2(z_{x,y}) = z_{x,y-1} - 2z_{x,y} + z_{x,y+1} \quad (11)$$

$$d_c^3(z_{x,y}) = \frac{1}{\sqrt{2}} \left[z_{x-1,y-1} - 2z_{x,y} + z_{x+1,y+1} \right] \quad (12)$$

$$d_c^4(z_{x,y}) = \frac{1}{\sqrt{2}} \left[z_{x-1,y+1} - 2z_{x,y} + z_{x+1,y-1} \right] \quad (13)$$

Substituting (7) and (8) in (5), using the logarithm function and performing some manipulations, M_1 , M_2 can be safely dropped. The maximization of this posterior probability distribution is equivalent to the following regularized minimum problem

$$\hat{\boldsymbol{z}} = \arg\min \lambda \left\| \boldsymbol{Q}(\boldsymbol{g} - \boldsymbol{A}\boldsymbol{z} - \boldsymbol{B}) \right\|^2 + \sum_{x,y} \sum_{c \in C} \rho(d_c(z_{x,y})) \quad (14)$$

where λ is called as the regularization parameter.

2.3 Solution Method

A gradient descent optimization method is used for the minimum problem in (14). Differentiating the cost function with respect to $\boldsymbol{z}$, we have

$$\boldsymbol{r} = -\boldsymbol{A}^T \boldsymbol{Q}^T \boldsymbol{Q}(\boldsymbol{g} - \boldsymbol{A}\boldsymbol{z} - \boldsymbol{B}) + \lambda \boldsymbol{r}' \quad (15)$$

where $\boldsymbol{r}'$ is the derivative of the regularization term. Then, the desired image is solved by employing the successive approximations iteration

$$\hat{\boldsymbol{z}}_{n+1} = \hat{\boldsymbol{z}}_n - \beta_n \boldsymbol{r}_n \quad (16)$$

where n is the iteration number, β_n is the step size.

2.4 Parameter Determination

In order to use the observation model (2), $\boldsymbol{A}$ (gains) and $\boldsymbol{B}$ (biases) should be first determined. It is easily understood that the gain and bias should be respectively 1 and 0 for healthy pixels. For dead pixel in image inpainting, the gain can be regarded as 0 and the bias the pixel value. For the destriping problem, the parameters of pixels in a row or a column are often assumed to be the same. We use the moment matching method (Gadallah et al., 2000) to obtain the gains and biases of the stripe pixels Therefore, the moment matching method is a special case of the proposed algorithm with $\lambda \to \infty$ and $\boldsymbol{Q}$ being a unit matrix in equation (14).

The matrix $\boldsymbol{Q}$ is diagonal and its elements represent the reciprocal of the noise standard deviation in different pixel locations. For convenience, we scale the element values to the range of 0~1. The difference caused by the scaling can be balanced by λ (λ is determined heuristically). For all the healthy pixels, the corresponding elements are set as the maximum value 1. On the contrary, the elements should be 0 for dead pixels because they do not have any correlation with the true scene. The elements of other bad pixels are between 0 and 1, and they correlate with the local activity level, the validity of moment matching and so on. Generally, we can select small element values to recovery the information from the neighbors using the prior constraint. On the other hand, larger element values should be chosen for sharp regions in order to retain the high-frequency information. We use the standard deviation as the activity measure, and a simple linear function is employed to determine element values.

3. EXPERIMENTAL RESULTS

3.1 Destriping Experiments

The proposed algorithm was tested for destriping on images of the Moderate Resolution Imaging Spectrometer (MODIS) aboard the Terra and Aqua platforms. The Terra MODIS data used in this paper was acquired on December 31, 2007, and the Aqua MODIS data was acquired on December 28, 2003. Sections of size 400×400 were extracted from the original images as experimental data. For calculation and display convenience, the original data are coded to an 8-byte scale. The original images and destriped results of Terra and Aqua are, respectively, shown in Figure 1 and
Figure 2. It can be seen that the moment matching method can greatly improve the image quality, but there are still considerable radiance fluctuations within the resulting image. The proposed algorithm, however, provides a much more robust destriping from the visual perspective.

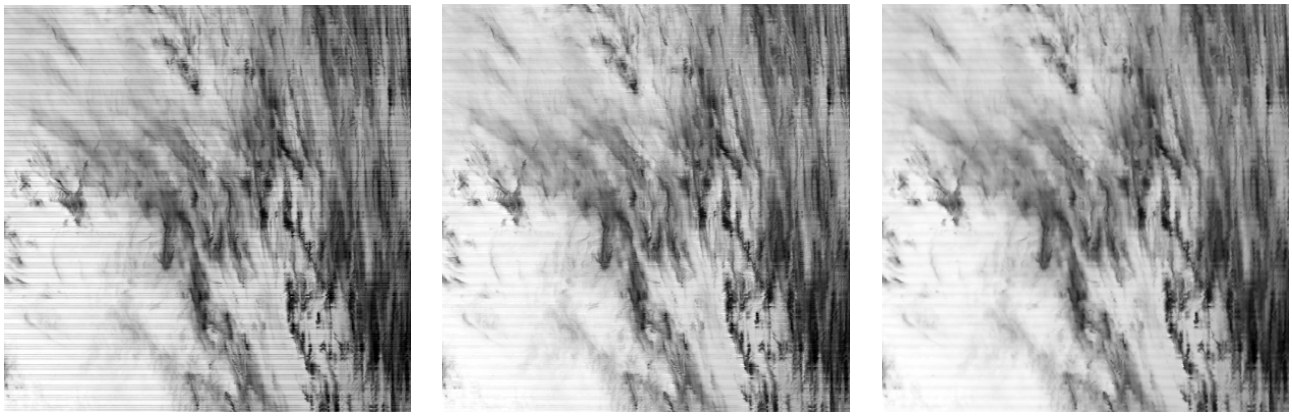

(a) original image (b) moment matching (c) the proposed algorithm

Figure 1. Destriped results of the Terra MODIS image.

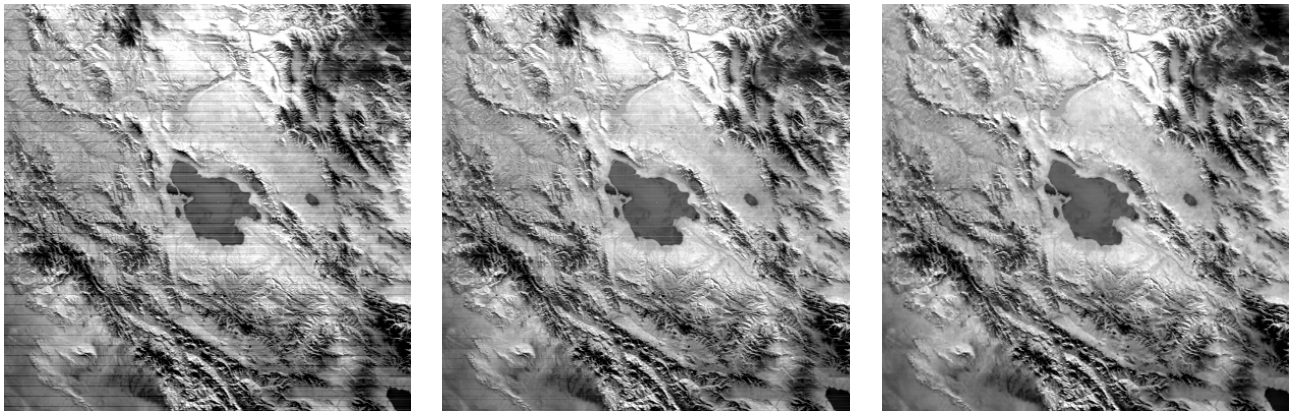

(a) original image (b) moment matching (c) the proposed algorithm

Figure 2. Destriped results of the Aqua MODIS image.

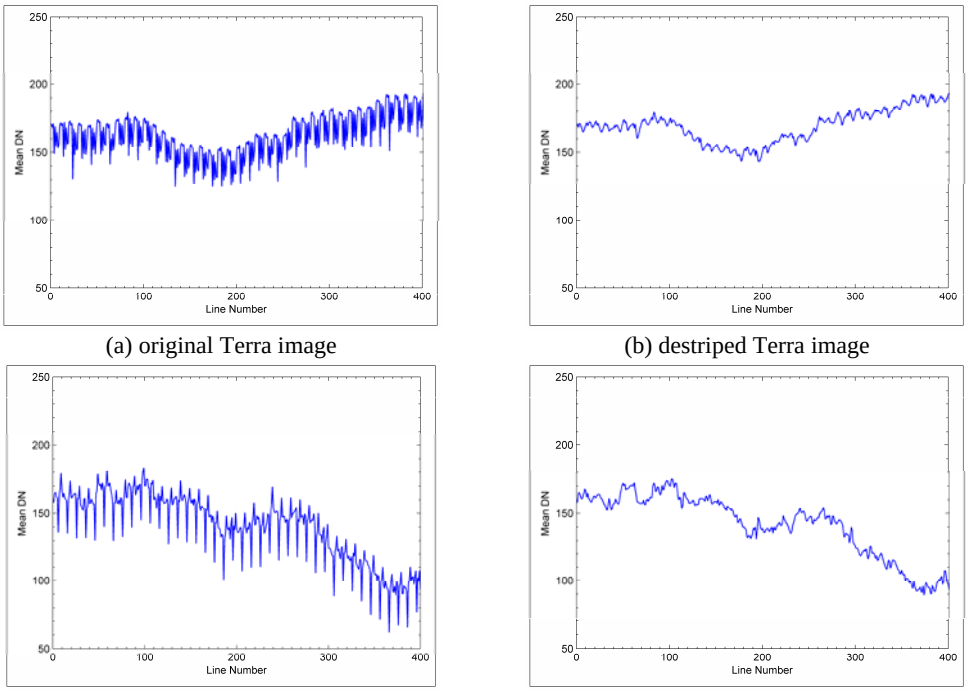

(a) original Terra image (b) destriped Terra image

(c) original Aqua image (d) destriped Aqua image

Figure 3. Mean cross-track profiles of the original and destriped MODIS images.

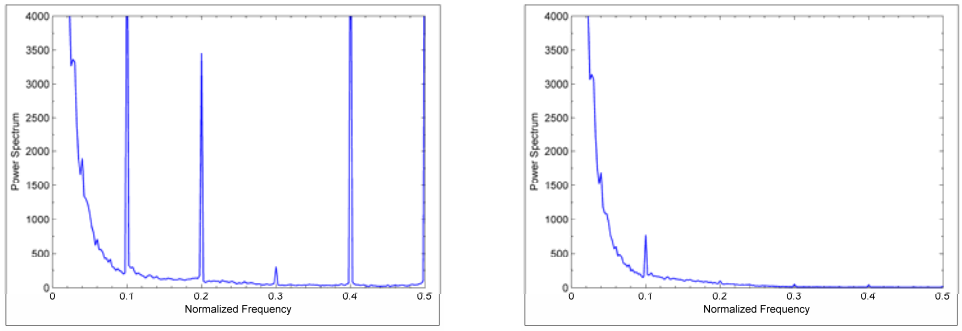

(a) original Terra image (b) destriped Terra image

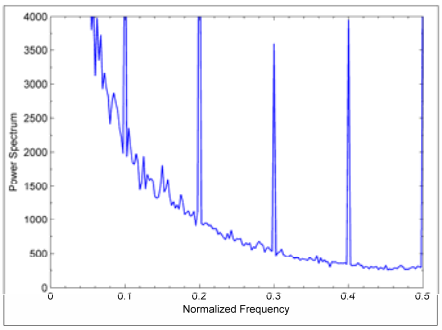

(c) original Aqua image

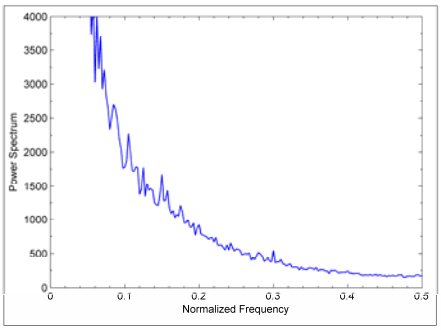

(d) destriped Aqua image

Figure 4. Mean column power spectrums of the original and destriped MODIS images.

Figure 3 shows the mean cross-track profiles of the original images and the destriped results using the proposed algorithm. It can be seen that the rapid fluctuations in the original data are strongly reduced in the destriped images. The mean column power spectrums of the original and destriped images are shown in
Figure 4. For better visualization of noise reduction, very high spectral magnitudes are not plotted. It is easily recognized that the value of the power spectrum of the frequency components where the pulses exist has been strongly reduced in the destriped images.

The inverse coefficient of variation (ICV) and ratio of noise reduction (NR) are employed to take the quantitative analysis. The ICV index (Nichol and Vohora, 2004; Rakwatin et al., 2007; Smith and Curran, 2000) is defined as

$$\mathrm{ICV} = \frac{R_a}{R_{sd}} \tag{17}$$

where R_a is the signal response of a homogeneous image region and is calculated by averaging the pixels within a window of a given size; R_{sd} refers to the noise components estimated by calculating the standard deviation of the pixel. In our experiments, we selected two 10×10 homogeneous regions for the ICV evaluation. The NR index (Chen et al., 2003; Rakwatin et al., 2007) is used to evaluate the image in the frequency domain. It is defined by

$$\mathrm{NR} = \frac{N_0}{N_1} \tag{18}$$

where N_0 is the power of the frequency components produced by stripes in the original image, and N_1 stands for that in the destriped image. N_0 and N_1 can be calculated by

$$N_i = \sum_{\wp} P_i(D) \tag{19}$$

where $P_i(D)$ is the averaged power spectrum down the columns of an image with D being the distance from the origin in Fourier space, and $\wp$ is the stripe noise region of the spectrum. The ICV and NR evaluation results are, respectively, shown in Table 1 and
Table 2. The proposed algorithm always obtains the best results in the several destriping methods (Butterworth filtering, moment matching and histogram matching).

		Original	Butterworth	Moment	Histogram	Proposed
Terra Band 28	Sample1	24.08	27.26	39.32	43.93	46.79
	Sample2	17.27	23.93	21.82	21.49	25.87
Aqua Band 30	Sample1	7.94	14.49	24.42	22.72	26.83
	Sample2	9.66	15.74	21.03	24.86	30.31

Table 1. ICVs of the original and destriped MODIS data

	Original	Butterworth	Moment	Histogram	Proposed
Terra Band 28	1.00	4.39	15.96	17.71	25.81
Aqua Band 30	1.00	4.26	4.82	5.05	7.56

Table 2. NRs of the original and destriped MODIS data

3.2 Inpainting Experiments

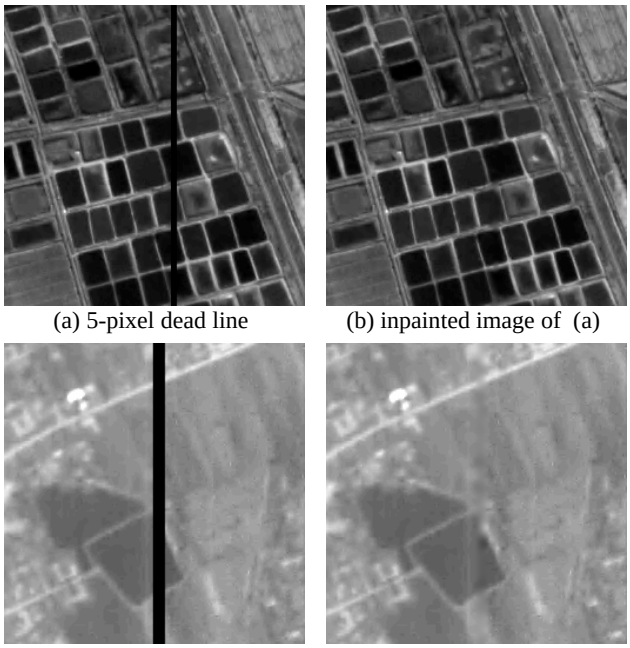

(a) 5-pixel dead line (b) inpainted image of (a)

(c) 8-pixel dead line (d) inpainted image of (c)

Figure 5. Inpainting experimental results of CBERS images for the recovery of vertical dead lines.

Figure 5 shows the inpainting experiments of CBERS (China-Brazil Earth Resource Satellite) images for the recovery of vertical dead lines.
Figure 5(a) and
Figure 5(c) are contaminated

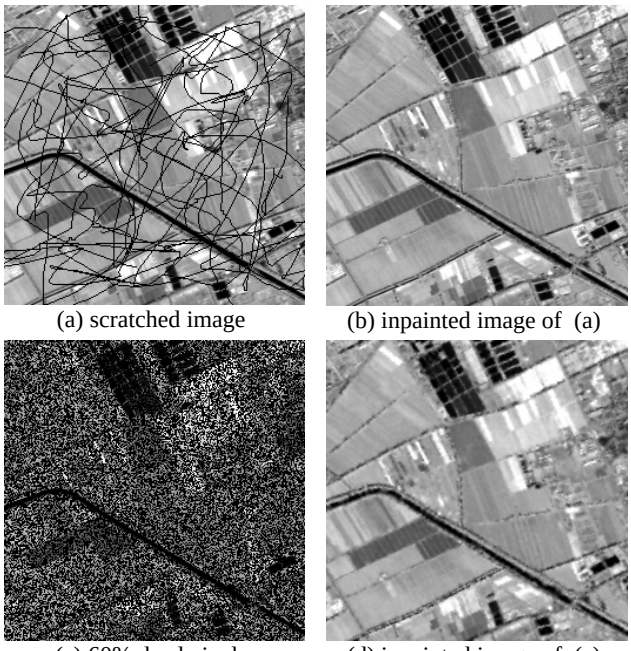

(a) scratched image (b) inpainted image of (a)

(c) 60% dead pixels (d) inpainted image of (c)

Figure 6. Inpainting experimental results of IKONOS images.

by dead lines of 5-pixel width and 8-pixel width respectively. It is known that the conventional methods are not employable for such wide dead lines.

Figure 5(b) and
Figure 5(d) are the corresponding inpainted results using the proposed algorithm. Although the lost information cannot be completely recovered, the visual quality of the resulted images is very convincing.
Figure 6(a) is a simulated image contaminated by some scratches, and
Figure 6(b) shows the inpainted result. It is seen that most of the lost information has been recovered.
Figure 6(c) assumes the image is contaminated by randomly distributed dead pixels whose percentage is 60%. The inpainted result is shown in
Figure 6(d). This experiment validates the strong performance of the proposed algorithm. Although such random distribution of dead pixels is not very familiar to many remote sensing users, it is often met in remote sensing pre-processing before data distribution.

4. CONCLUSIONS

In this paper, we present a maximum *a posteriori* (MAP) based algorithm for both destriping and inpainting problems. The main advantage of this algorithm is that it can constrain the solution space according to *a priori* constraint during the destriping and inpainting processes. In the destriping experiments, we tested the proposed algorithm on Terra and Aqua MODIS images. The quantitative analysis showed that the proposed algorithm provides more assurance of desired results than the conventional destriping methods. In the inpainting experiments, the recovery of vertical, scratched and random dead pixels are respectively tested. Experimental results validated that the contaminated images can be noticeably improved by implementing the proposed algorithm.

REFERENCES:

Algazi, V.R. and G. E. Ford, 1981. Radiometric equalization of nonperiodic striping in satellite data. Computer Graphics and Image Processing, 16(3): 287-295.

Bertalmio, M., Sapiro, G., Caselles, V. and Ballester, C., 2000. Image inpainting, the ACM SIGGRAPH Conference on Computer Graphics, New Orleans, LA, pp. 417-424.

Borman, S. and Stevenson, R., 1998 Spatial Resolution Enhancement of Low-Resolution Image Sequences: A Comprehensive Review with Directions for Future Research. Report, Laboratory for Image and Signal Analysis (LISA), University of Notre Dame,.

Chen, J., Shao, Y., Guo, H., Wang, W. and Zhu, B., 2003. Destriping CMODIS data by power filtering. IEEE Transactions on Geoscience and Remote Sensing 41(9): 2119-2124.

Chen, J.S., Lin, H., Shao, Y. and Yang, L.M., 2006. Oblique striping removal in remote sensing imagery based on wavelet transform. International Journal of Remote Sensing, 27(8): 1717-1723.

Ferrari, P.A., Frigessi, A. and de Sa, P.G., 1995. Fast Approximate Maximum a Posteriori Restoration of Multicolour

Images. Journal of the Royal Statistical Society. Series B (Methodological), 57(3): 485-500.

Gadallah, F.L., Csillag, F. and Smith, E.J.M., 2000. Destriping multisensor imagery with moment matching. International Journal of Remote Sensing, 21(12): 2505-2511.

Hamza, A.B. and Krim, H., 2004. A variational approach to maximum a posteriori estimation for image denoising. Lecture Notes in Computer Science: 19-33.

Horn, B.K.P. and Woodham, R.J., 1979. Destriping Landsat MSS images by histogram modification. Comput. Graph. Image Process, 10(1): 69-83.

Nichol, J.E. and Vohora, V., 2004. Noise over water surfaces in Landsat TM images. International Journal of Remote Sensing, 25(11): 2087-2093.

Poros, D.J. and Peterson, C.J., 1985. Methods for destriping Landsat Thematic Mapper images- A feasibility study for an online destriping process in the Thematic Mapper Image Processing System(TIPS). Photogrammetric Engineering and Remote Sensing, 51: 1371-1378.

Rakwatin, P., Takeuchi, W. and Yasuoka, Y., 2007. Stripe noise reduction in MODIS data by combining histogram matching with facet filter. IEEE Transactions on Geoscience and Remote Sensing, 45(6): 1844-1856.

Ratliff, B.M. et al., 2007. Dead pixel replacement in LWIR microgrid polarimeters. Optics Express, 15(12): 7596-7609.

Schultz, R.R. and Stevenson, R.L., 1996. Extraction of high-resolution frames from video sequences. IEEE Transactions on Image Processing, 5(6): 996-1011.

Shen, H., Ng, M.K., Li, P. and Zhang, L., 2007, doi:10.1093/comjnl/bxm028. Super Resolution Reconstruction Algorithm to MODIS Remote Sensing Images. The Computer Journal.

Shen, H., Zhang, L., Huang, B. and Li, P., 2007. A MAP Approach for Joint Motion Estimation, Segmentation, and Super Resolution. IEEE Transactions on Image Processing, 16(2): 479-490.

Smith, G.M. and Curran, P.J., 2000. Methods for estimating image signalto-noise ratio. Advances in Remote Sensing and GIS Analysis, P. M. Atkinson and N. J. Tate, Eds. Hoboken, NJ:Wiley,: 61-74.

Torres, J. and Infante, S.O., 2001. Wavelet analysis for the elimination of striping noise in satellite images. Optical Engineering, 40(7): 1309-1314.

Wegener, M., 1990. Destriping multiple sensor imagery by improved histogram matching. International Journal of Remote Sensing, 11(5): 859 - 875.

ACKNOWLEDGEMENTS

This research are funded by Key Laboratory of Mine Spatial Information Technologies of SBSM (State Bureau of Surveying and Mapping) NO. KLM2008 and Digital Land Key Lab of Jiangxi Province.